Elasticity of Cylindrical Black Holes

Conrad Pearson

Advisor: Scott Fraser

Physics Department

California Polytechnic State University, San Luis Obispo

Winter 2016

Abstract

Black holes are regions of strong gravity, and are often regarded as behaving like drops of fluid. When this line of thought is applied to cylindrical black holes (black cylinders), a mapping can be made between known instabilities for black cylinders and ordinary fluid cylinders. However, this known correlation is increasingly less accurate for lower spatial dimensions, and I seek to correct this discrepancy in this thesis. By considering soft solids instead of pure fluids, elastic energy can be included, which brings us closer to a direct comparison. In improving this mapping, it becomes possible to better understand the behavior of black cylinders through experiments with soft cylinders, which are easily observed in the laboratory. An extended version of this thesis will be available on the arXiv.org research article repository.

Introduction and Motivation

A spherical black hole is a famous example of strong gravity and is described by the geometry of space. The following geometry describes a black hole in the shape of a cylinder:

$$ds^2 = \frac{dr^2}{f} + r^2 d\Omega^2 + dz^2, \qquad f = 1 - \left(\frac{R_0}{r}\right)^{d-3}, \tag{1}$$

where d is the number of spatial dimensions. In four spatial dimensions ($d = 4$), the angular quantity is $d\Omega^2 = d\theta^2 + \sin^2\theta d\phi^2$, and in higher dimensions, $d\Omega^2$ contains additional angles. The surface formed by $r = R_0$ is inescapable for particles that fall inside it, and is the strong gravity surface of a black hole. The particular geometry (1) is actually a stack of spherical black holes. The stack extends in the extra dimension z (meaning there is a minimum of 4 dimensions), forming the black cylinder. If we visualize this as a cylinder in three dimensions, thin disk-shaped slices would be the black holes (and the black holes are actually spheres instead of disks). The black cylinder is illustrated in Figure 1, which also shows a perturbation of it.

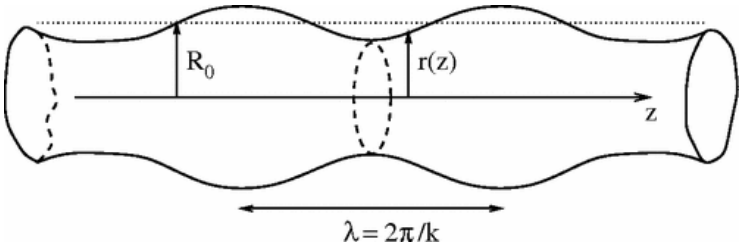

Figure 1: A cylinder with unperturbed radius $r = R_0$. The perturbed surface has radius $r(z)$ and the perturbation has wavelength λ. This figure has been borrowed from [3].

It is possible that an observed spherical black hole could actually be a slice, as described above, of a higher dimensional black cylinder. Experiments are currently looking for evidence of extra dimensions, although they have yet to be detected.

The black cylinder's surface area A is related to the energy E contained in the surrounding space. As found in

[1], their perturbations are related by (2),

$$\delta E = \gamma \delta A, \qquad \gamma = \frac{d-3}{16\pi G R_0}. \tag{2}$$

Here G is the gravitational constant, and I have used standard units, in which the speed of light is 1. As originally suggested by Smarr [2], equation (2) is comparable to the behavior of an ordinary fluid, with γ being identified as the effective surface tension of the black cylinder, in analogy with the surface tension γ (surface energy per unit area) of an ordinary fluid.

In this thesis, I seek to expand upon this remarkable connection between fluids and black cylinders by considering soft solids with an elastic shear modulus μ (also called the modulus of rigidity), which is similar to the stiffness in a spring. My goal is to improve the connection between ordinary fluid cylinders and black cylinders. Unlike the black cylinder, soft solids are laboratory materials that can be observed and more easily understood. Thus, the better we understand the connection between these objects, the better we understand black cylinders, and in the future, this may lead to a better understanding of strong gravity.

Known Instabilities of Cylinders

Both fluid cylinders and black cylinders have known instabilities that act to change the energy of the cylinder by changing the surface area, as in equation (2). For a ordinary fluid, the perturbed cylinder seeks to minimize its energy, and typically breaks into individual droplets. This effect can be seen in the breakup of water dripping from a faucet. For a perturbed black cylinder, the final evolved shape (after the initial perturbation) has been an ongoing area of investigation, and I will return to this point in the concluding section of this thesis. Each perturbation is described by a wavelength λ and wavenumber $k = 2\pi/\lambda$, as shown in Figure 1. For convenience, I use the wavenumber k. Whether or not the instability will occur is dependent on the unperturbed cylinder radius R_0 and the wavenumber k of the perturbation. For k less than a critical value k_c, the cylinder is unstable. For a fluid cylinder, the critical wavenumber is [3],

$$k_c R_0 = \sqrt{d-2}. \tag{3}$$

For the black cylinder, a perturbation that propagates inwards from infinity will cause an instability on the surface of the black cylinder. This too has a stability condition defined by the wavenumber k and the radius R_0 of the black cylinder. The critical value k_c has been calculated numerically in [3, 4] for many possible dimensions d. At large values of d, the asymptotic formula is [5],

$$k_c R_0 = \sqrt{d-3}\left[1 - \frac{1}{2(d-3)}\right]. \tag{4}$$

Equations (3) and (4) are similar in form, and they agree well for large values of the dimension d, where both expressions approach the square root of the dimension, $\sqrt{d}$. However, at lower dimensions, the agreement

becomes less accurate: for a black cylinder, at the lowest values of d (4, 5, 6) the calculated values of $k_c R_0$ (0.876, 1.27, 1.58) are noticeably smaller than the fluid values (1.41, 1.73, 2.00) given by (3). Introducing a new property could correct this discrepancy, so in the next section, I generalize the pure fluid considered above to a soft solid with a small nonzero elastic modulus μ.

My Results for the Soft Solid Instability

To improve the agreement between equations (3) and (4), I examine soft solids as a replacement for (3). Soft solids, such as gels, have properties of both fluids and solids. The soft solid that I examine has both a surface tension γ and an elastic modulus μ (for an ordinary fluid, $\mu = 0$). The elastic modulus μ is analogous to the elastic constant of a spring. Deformations of the soft cylinder always add to its elastic energy. This means the elastic modulus will oppose the energy minimizing changes caused by the surface tension.

The instability for soft solids has been previously found in $d = 3$ dimensions [6]. In this section, I summarize my generalization of [6] to higher dimensions ($d \geq 4$). This calculation requires minimizing the elastic energy $E_{elastic}$ of the cylinder, which is (5),

$$E_{elastic} = \mu \int\int \omega_{d-2} r^{d-2} \Big[\Big(\frac{\partial S_r}{\partial r}\Big)^2 + \Big(\frac{\partial S_z}{\partial z}\Big)^2 + (d-2)\frac{(S_r)^2}{r^2} + \frac{1}{2}\Big(\frac{\partial S_r}{\partial z} + \frac{\partial S_z}{\partial r}\Big)^2 - p\Big(\frac{\partial S_r}{\partial r} + (d-2)\frac{S_r}{r} + \frac{\partial S_z}{\partial z}\Big)\Big] dr dz. \tag{5}$$

The variables S_r and S_z describe displacements (deformations) along the radius and the length of the tube, in the directions (r, z) shown in Figure 1. The quantity ω_{d-2} is the surface area of a d-dimensional sphere with unit radius. Finally, the variable p represents the Lagrange multiplier which enforces the incompressibility condition (6),

$$\frac{\partial S_r}{\partial r} + (d-2)\frac{S_r}{r} + \frac{\partial S_z}{\partial z} = 0. \tag{6}$$

To minimize the energy of the system I apply Lagrange's equations (7) for S_r and S_z to the integrand of (5) which I'll call the Lagrangian ($\mathcal{L}$),

$$\frac{\partial \mathcal{L}}{\partial f} = \sum_{x_i = r,z} \frac{\partial}{\partial x_i}\Big(\frac{\partial \mathcal{L}}{\partial(\frac{\partial f}{\partial x_i})}\Big) \tag{7}$$

This will result in two partial differential equations (8, 9), which are known in elasticity as Cauchy Poisson equations:

$$\mu\Big[2\frac{\partial^2 S_z}{\partial z^2} + \frac{\partial}{\partial r}\Big(\frac{\partial S_r}{\partial z} + \frac{\partial S_z}{\partial r}\Big) + \frac{d-2}{r}\Big(\frac{\partial S_r}{\partial z} + \frac{\partial S_z}{\partial r}\Big)\Big] - \frac{\partial p}{\partial z} = 0 \tag{8}$$

$$\mu\Big(\frac{\partial^2 S_r}{\partial z^2} - \frac{\partial}{\partial r}\frac{\partial S_z}{\partial z}\Big) - \frac{\partial p}{\partial r} = 0. \tag{9}$$

To reduce these equations to an ordinary differential equation, I apply the incompressibility condition, and the

fact that the z dependence of the variables (S_r , S_z , p) must take on the same form as the perturbation (10):

$$S_r = \sigma(r)e^{ikz}, \qquad S_z = w(r)e^{ikz}, \qquad p - (d-2)\frac{\gamma}{R_0} = q(r)e^{ikz}. \tag{10}$$

This gives a fourth order ordinary differential equation (11),

$$\Big(\Phi - k^2\Big)^2 \sigma(r) = 0, \qquad \Phi = \frac{\partial^2}{\partial r^2} + \frac{(d-2)}{r}\frac{\partial}{\partial r} - \frac{(d-2)}{r^2}. \tag{11}$$

To solve this equation, I use two types of solutions: two solutions result from applying the operator once, then the other two result from applying the operator to those solutions. The first type of equation, $(\Phi - k^2)\sigma = 0$, is a modified Bessel's equation, thus has solutions with Bessel's functions I_ν and K_ν:

$$\sigma_1 = \alpha r^{-(\frac{d-3}{2})} I_{\frac{d-1}{2}}(kr), \qquad \sigma_2 = \alpha r^{-(\frac{d-3}{2})} K_{\frac{d-1}{2}}(kr), \tag{12}$$

where α is a constant. The second type of solution satisfies equation (13):

$$\Big(\Phi - k^2\Big)\sigma(r) = \beta\sigma_1(r), \tag{13}$$

where β is a constant. To solve this I use the Wronskian method, also known as variation of parameters [8]. This means the solution will have the form (14),

$$\sigma_3(r) = C_1(r)\sigma_1(r) + C_2(r)\sigma_2(r), \tag{14}$$

where C_1, C_2 satisfy equation (15),

$$\begin{bmatrix} \sigma_1(r) & \sigma_2(r) \\ \frac{d}{dr}\sigma_1(r) & \frac{d}{dr}\sigma_2(r) \end{bmatrix} \begin{bmatrix} \frac{d}{dr}C_1(r) \\ \frac{d}{dr}C_2(r) \end{bmatrix} = \begin{bmatrix} 0 \\ \beta\sigma_1(r) \end{bmatrix}. \tag{15}$$

Solving for C_1, C_2 results in (16),

$$\sigma_3 = -\beta r^{-(\frac{d-3}{2})} I_{\frac{d-1}{2}}(kr) \int_r^{R_0} r' K_{\frac{d-1}{2}}(kr') I_{\frac{d-1}{2}}(kr')dr' + \beta r^{-(\frac{d-3}{2})} K_{\frac{d-1}{2}}(kr) \int_r^{R_0} r' I^2_{\frac{d-1}{2}}(kr')dr'. \tag{16}$$

The solutions for σ_2 and the solution that would result from replacing σ_1 in (13) with σ_2 both diverge for $r = 0$. This means they are unphysical and are not included in the overall solution. Thus the solution for σ is a linear combination of σ_1 and σ_3,

$$\sigma = \frac{\alpha}{r^{\frac{d-3}{2}}} I_{\frac{d-1}{2}}(kr) - \frac{\beta}{r^{\frac{d-3}{2}}}\left[I_{\frac{d-1}{2}}(kr) \int_r^{R_0} r' K_{\frac{d-1}{2}}(kr') I_{\frac{d-1}{2}}(kr')dr' - K_{\frac{d-1}{2}}(kr) \int_r^{R_0} r' I^2_{\frac{d-1}{2}}(kr')dr' \right] \tag{17}$$

To make use of this solution, I will look at the boundary conditions. This system will have boundary conditions based on the behavior at the surface. First I look at the area variation at the surface (18),

$$\delta A = \int \kappa \, dA_S \, dN. \tag{18}$$

In this equation dA_S is the differential surface element of the cylinder. dN is a small quantity along the normal vector $\hat{n}$ (19),

$$\hat{n} = \frac{1}{\Big(1 + r'(z)^2\Big)^{1/2}}\hat{r} - \frac{r'(z)}{\Big(1 + r'(z)^2\Big)^{1/2}}\hat{z}. \tag{19}$$

κ is the trace of the extrinsic curvature, and is defined in (20),

$$\kappa = \frac{d-2}{r(z)\Big(1 + r'(z)^2\Big)^{1/2}} - \frac{r''(z)}{\Big(1 + r'(z)^2\Big)^{3/2}}. \tag{20}$$

The area variation δA can be simplified by assuming the perturbation is small relative to the radius, resulting in (21),

$$\delta A = \omega_{d-2}\int r(z)^{d-2}\left[(d-2)\Big(\frac{1}{R_0} - \frac{S_r}{R_0^2}\Big) - \frac{\partial^2 S_r}{\partial z^2}\right]\delta S_r\, dz. \tag{21}$$

As in (2), this will contribute energy based on the surface tension, $\gamma\delta A$.

Then, I look at the boundary energy at the surface (22),

$$\delta\mathcal{E}_b = \omega_{d-2}\int r^{d-2}\left[\frac{\partial\mathcal{L}}{\partial(\frac{\partial S_r}{\partial r})}\delta S_r + \frac{\partial\mathcal{L}}{\partial(\frac{\partial S_z}{\partial r})}\delta S_z\right]dz. \tag{22}$$

This arises as the boundary term from integration by parts of the variation of the elastic energy. Plugging in the Lagrangian, I get (23),

$$\delta\mathcal{E}_b = \omega_{d-2}\int r(z)^{d-2}\left[\Big(2\mu\frac{\partial S_r}{\partial r} - p\Big)\delta S_r + \mu\Big(\frac{\partial S_r}{\partial z} + \frac{\partial S_z}{\partial r}\Big)\delta S_z\right]dz. \tag{23}$$

For the critical condition of the instability, the sum of the boundary energy and the surface tension times the area variation must be zero at the surface, where $r(z) = R_0 + S_r$. This results in two boundary conditions (24, 25):

$$-\gamma\left[(d-2)\frac{S_r}{R_0^2} + \frac{\partial^2 S_r}{\partial z^2}\right] + 2\mu\frac{\partial S_r}{\partial r} - \Big(p - (d-2)\frac{\gamma}{R_0}\Big) = 0, \tag{24}$$

$$\frac{\partial S_r}{\partial z} + \frac{\partial S_z}{\partial r} = 0. \tag{25}$$

For the cylinder to be unstable, the left hand side of (24) must be less than zero. By applying these boundary conditions to the solution for S_r (17), I find a relation (26) among the surface tension γ, the elastic modulus μ, and the perturbation wavenumber k,

$$\frac{\gamma}{\mu R_0} = \frac{2}{(d-2) - (kR_0)^2}\left[\frac{2kR_0 I_{(d-3)/2}(kR_0)}{I_{(d-1)/2}(kR_0)} - (d-2)\right]. \tag{26}$$

My result (26) is plotted as a curve in Figure 2. The curve forms the cutoff for the instability: perturbed cylinders corresponding to points below the curve are unstable, and perturbed cylinders corresponding to points outside the curve are stable. From this, it is clear that a nonzero elastic modulus μ will result in a lower value of $k_c R_0$.

This means that by matching equation (4), and the values of $k_c R_0$ listed below it, to the curve in Figure 2, I find a correspondence between soft solids and black cylinders, and I find the elastic modulus μ for black cylinders. In the next section, I obtain this value of μ by using the part of the curve in Figure 2 near the cutoff point for a pure fluid, $k_c R_0 = \sqrt{d-2}$.

Matching My Results to the Black Cylinder

To find a simpler form for my result (26), I evaluate the Bessel functions using some well-known expansions. First, I expand about the point $k_c R_0 = \sqrt{d-2}$. I assume a large number of dimensions d, and use asymptotic forms of the Bessel functions. This gives (27),

$$\frac{\mu R_0}{\gamma} = \frac{\sqrt{d-2} - k_c R_0}{\sqrt{d}}. \tag{27}$$

For the black cylinder, I perform a similar expansion of (4) about the point $kR_0 = \sqrt{d-2}$ for high dimensions. This gives (28),

$$\sqrt{d-2} - k_c R_0 = \frac{1}{\sqrt{d}}. \tag{28}$$

Now substituting this into (27) and substituting γ from (2) gives the effective value of μ for black cylinders (29),

$$\mu = \frac{1}{16\pi G {R_0}^2}. \tag{29}$$

This result bears similarity to γ in (2) and is rather simple, which is exactly what was desired. However, it is important to note that the expression for the elastic modulus μ will be more complicated at lower dimensions; the simplified form in (29) is the behavior at higher dimensions. For lower dimensions, I performed this calculation numerically. The result is shown in Figure 3, which also illustrates the growth towards the asymptotic value (29).

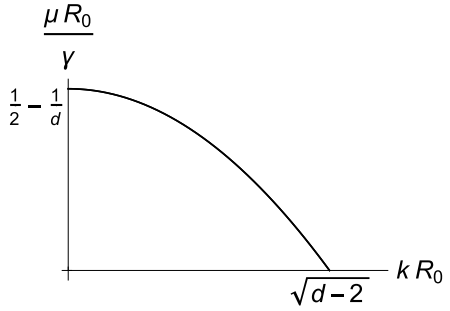

Figure 2: Instability curve for a soft solid cylinder in d spatial dimensions. Perturbed cylinders corresponding to points below the curve are unstable.

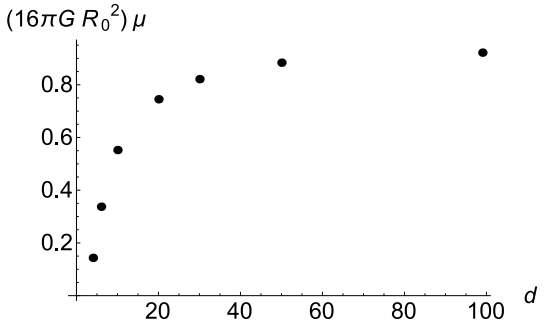

Figure 3: The elastic modulus μ for black cylinders in d dimensions, from numerically matching Figure 2 to the values of $k_c R_0$ listed below (4).

Conclusion and Extensions

I have accomplished my goal of improving the mapping between fluid cylinders and black cylinders, by including a material property, the elastic modulus μ. This work provides a new understanding of the behavior of black cylinders, through a comparison to soft solids, which can be directly observed in experiments.

So far, my results apply to a black cylinder of infinite length, however it may also be possible to use Figure 2 to match an elastic modulus to black cylinders with finite length L. This new application of my work involves examining the cylinder's final evolved shape (after the initial perturbation). The final evolution of a perturbed unstable black cylinder was found in [5] to be a stable periodic shape (rather than a set of disconnected spherical black holes, analogous to fluid droplets). This is shown in Figure 4.

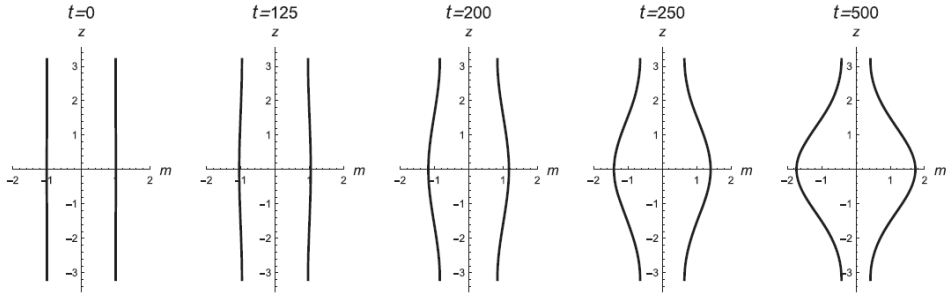

Figure 4: The result of [5], showing the time evolution of a black cylinder with radial size m. The stable equilibrium shape has formed by time $t = 500$.

The stable shape of the black cylinder in Figure 4 appears to be consistent with the stable evolved equilibrium shapes of perturbed soft solids in laboratory experiments [6] and in numerical solutions [7]. The laboratory results are shown in Figure 5. This suggests that an application of my work to finite black cylinders is possible.

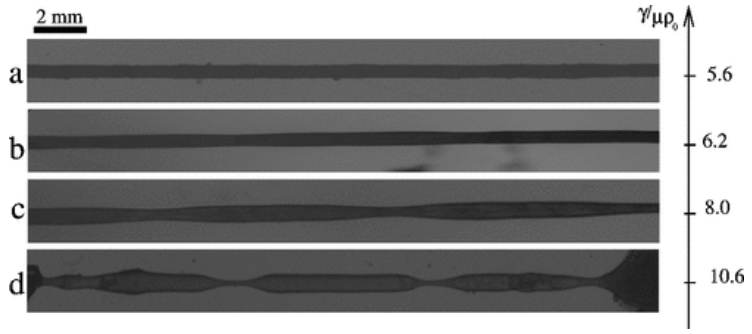

Figure 5: The experiments of [6], showing the stable evolved equilibrium shapes of perturbed unstable cylinders (b, c, d) with initial radius $\rho_0 = R_0$, and different elastic moduli μ. Cylinder (a) is stable due to its high elastic modulus.

References

[1] P. Townsend and M. Zamaklar, *The first law of black brane mechanics*, Class. Quant. Grav. **18**, 5269 (2001).

[2] L. Smarr, *Mass formula for Kerr black holes*, Phys. Rev. Lett. **30**, 71 (1973).

[3] V. Cardoso and O. Dias, *Rayleigh-Plateau and Gregory-Laflamme instabilities of black strings*, Phys. Rev. Lett. **96**, 181601 (2006).

[4] V. Asnin, D. Gorbonos, S. Hadar, B. Kol, M. Levi, and U. Miyamoto, *High and low dimensions in the black hole negative mode*, Class. Quant. Grav. **24**, 5527 (2007).

[5] R. Emparan, R. Suzuki, and K. Tanabe, *The large D limit of general relativity*, J. High Energy Phys. **1306**, 9 (2013).

[6] S. Mora, T. Phou, J. Fromental, L. Pismen, and Y. Pomeau, *Capillarity driven instability of a soft solid*, Phys. Rev. Lett. **105**, 214301 (2010).

[7] M. Taffetani and P. Ciarletta, *Beading instability in soft cylindrical gels with capillary energy*, J. Mech. Phys. Solids **81**, (2015).

[8] C. Ross, *Differential Equations, An Introduction with Mathematica*, Springer (2010).